Environ Sci Technol (2010) shortened versio

DATASET · JANUARY 2014

READS
69

7 AUTHORS, INCLUDING:

Carles Pellicer-Nàcher
Veolia Water Technologies AB - Hydrotech
13 PUBLICATIONS **167** CITATIONS
SEE PROFILE

Susanne Lackner
Karlsruhe Institute of Technology
31 PUBLICATIONS **428** CITATIONS
SEE PROFILE

Akihiko Terada
Tokyo University of Agriculture and Techn…
79 PUBLICATIONS **1,273** CITATIONS
SEE PROFILE

Barth F Smets
Technical University of Denmark
181 PUBLICATIONS **3,768** CITATIONS
SEE PROFILE

Environ. Sci. Technol. **2010,** *44,* 7628–7634

Sequential Aeration of Membrane-Aerated Biofilm Reactors for High-Rate Autotrophic Nitrogen Removal: Experimental Demonstration

CARLES PELLICER-NÀCHER,[†] SHENGPENG SUN,[†,‡] SUSANNE LACKNER,[†,⊥] AKIHIKO TERADA,[†,#] FRANK SCHREIBER,[§] QI ZHOU,[‡] AND BARTH F. SMETS*[,†]

Department of Environmental Engineering, Technical University of Denmark, Miljøvej building 113, 2800 Kongens Lyngby, Denmark, Department of Environmental Science and Engineering, Tongji University, 1239 Siping Road, Shanghai, P.R. China, and Max Planck Institute for Marine Microbiology, D-28359 Bremen, Germany

Received April 26, 2010. Revised manuscript received July 29, 2010. Accepted August 6, 2010.

One-stage autotrophic nitrogen (N) removal, requiring the simultaneous activity of aerobic and anaerobic ammonium oxidizing bacteria (AOB and AnAOB), can be obtained in spatially redox-stratified biofilms. However, previous experience with Membrane-Aerated Biofilm Reactors (MABRs) has revealed a difficulty in reducing the abundance and activity of nitrite oxidizing bacteria (NOB), which drastically lowers process efficiency. Here we show how sequential aeration is an effective strategy to attain autotrophic N removal in MABRs: Two separate MABRs, which displayed limited or no N removal under continuous aeration, could remove more than 5.5 g N/m^2/day (at loads up to 8 g N/m^2/day) by controlled variation of sequential aeration regimes. Daily averaged ratios of the surficial loads of O_2 (oxygen) to NH_4^+ (ammonium) (L_{O_2}/L_{NH_4}) were close to 1.73 at this optimum. Real-time quantitative PCR based on 16S rRNA gene confirmed that sequential aeration, even at elevated average O_2 loads, stimulated the abundance of AnAOB and AOB and prevented the increase in NOB. Nitrous oxide (N_2O) emissions were 100-fold lower compared to other anaerobic ammonium oxidation (Anammox)-nitritation systems. Hence, by applying periodic aeration to MABRs, one-stage autotrophic N removal biofilm reactors can be easily obtained, displaying very competitive removal rates, and negligible N_2O emissions.

Introduction

Membrane-aerated biofilm reactors (MABRs) seem ideally suited to support a one-stage nitritation-Anammox process: redox-stratified biofilms containing AOB and AnAOB can be grown on gas-permeable membranes with O_2 filling the membrane lumen and NH_4^+ and other substrates counter-diffusing from the liquid-biofilm interface. Since O_2 is supplied directly to the biofilm through a bubbleless membrane, O_2 transfer efficiency is enhanced, reducing diffusion limitations, ensuring biofilm integrity and avoiding stripping of nondesired gases. Furthermore, the installation of these membranes in rotating modules permits controlled biofilm shearing, further countering mass transfer limitations (*1*−*3*). These one-reactor systems have also proved to be more sustainable with regard to the emission of N_2O, a gas which has infrared radiative forcing 206 times that of CO_2 (*4, 5*). On the other hand, AnAOB have a low specific growth rate and high sensitivity toward common compounds such as methanol, dissolved oxygen (DO) and nitrite (NO_2^-), which could easily impair their cultivation in a process like the one presented here (*6, 7*).

Our previous laboratory-scale studies have shown that N removal might not be easily achieved in MABRs because of competition between AOB, NOB, and AnAOB for DO and NO_2^- (*8*−*10*). NOB populations can easily develop in the inner aerobic zones of the biofilm converting the NO_2^- generated by AOB to nitrate (NO_3^-), removing an essential substrate from AnAOB (*8*). Reactor conditions like operation at high pH and NH_4^+ concentrations (favoring high free ammonia concentrations), low DO concentrations, and temperatures between 30−33 °C can favor AOB growth over NOB (*11*−*13*) but may not control NOB in MABR biofilms because their presence at the biofilm base, once established, provides spatial protection.

Therefore, new approaches are needed to inhibit NOB activity in MABRs if completely autotrophic N removal is pursued. One approach is the joint inoculation of AnAOB and NOB, and exploiting their competition for the NO_2^- produced by AOB (*7*). The microbial community structure of the inoculum has also proven to affect the performance of these reactors. An inoculation dominated by slow-growing NOB such as *Nitrospira* instead of *Nitrobacter* positively impacts the nitritation efficiency in MABRs (*8*). Along the same lines, periodic aeration may be another approach to suppress NOB in MABRs. Because nitratation often lags nitritation (*14*), such operation might stimulate NO_2^- accumulation, and hence AnAOB growth. Moreover, the periodic imposition of anaerobic periods may limit the DO concentration for NOB and stimulate the decay of obligate aerobes. This aeration strategy has earlier proven to enhance NO_2^- accumulation in codiffusion SBR systems (*15*) and chemostats (*16*), although the mechanism for NOB inhibition remains unclear.

Here we provide detailed evidence on how sequential aeration can be used to initiate or improve autotrophic N removal in unoptimized MABRs. N mass balances and molecular community descriptors were derived to show that this operational strategy stimulates AnAOB activity, inhibits NOB activity, and hence increases N removal to high volumetric and surficial rates. Moreover, the effect of the aeration pattern on N_2O production was quantified.

Experimental Section

MABR Reactor. Experiments were conducted in two laboratory-scale MABRs (R1 and R2) constructed from Plexiglas and PVC tubing. Each reactor housed a module which supported 10 membrane bundles with 128 hollow-fibers each with a length of 30 cm and an inner/outer fiber diameter of 200/280 μm (Model MHF3504, polyethylene/polyurethane,

* Corresponding author phone: +45 4525 52230; fax: +45 4593 52850; e-mail: bfsm@env.dtu.dk.
[†] Technical University of Denmark.
[‡] Tongji University.
[§] Max Planck Institute for Marine Microbiology.
[⊥] Current Affiliation: Aquantis GmbH, Veolia Water Solutions & Technologies, Lise-Meitner-Str. 4a, 40878 Ratingen Germany.
[#] Current Affiliation: Department of Chemical Engineering, Tokyo University of Agriculture & Technology, Naka-cho 2-24-16, Koganei-shi, Tokyo, 184-8588, Japan.

10.1021/es1013467

Published on Web 09/03/2010

Mitsubishi Rayon Co., Ltd., Tokyo, Japan), yielding a total membrane surface area of 0.34 m^2. Air (O_2 source) was supplied in flow-through mode to the lower part of the membrane module. Pressure and gas flow rates in the membrane lumen were adjusted and monitored by pressure and gas flow gauges. Pressure loss in the membrane module was negligible. The length of aerobic and anaerobic phases was controlled by solenoid valves connected to an electronic timer (S-System S1321166−230, Electromatic, Denmark). The membrane module was attached to an electronic stirrer (RZR 2102, Heidolph, Germany), allowing rotation when desired. Reactor temperature could be controlled around 32 °C when necessary by a recirculating liquid coil (Julabo MB-5, Germany).

Complete mixing of the reactors was ensured through liquid recirculation (1 L/min) using an aquarium pump (1048−3148, Eheim, Germany) (section 2, SI). DO concentrations, pH, temperature, NH_4^+ and NO_3^- concentrations were monitored online with electrodes mounted in a flow cell placed in the recirculation line (CellOx 325, SentiX 41, Varion Plus 700IQ respectively. WTW, Germany). Electrode readings were displayed continuously and stored every tenth minute. The recorded data were cross-checked regularly with offline chemical analyses. The total volume of the system was 2.41 L. Further details about the setup are available in section 1 of the Supporting Information.

Feed/Operation. Feed composition was adopted from ref *6* and adjusted to match the desired influent NH_4^+ concentrations, which ranged from 530 to 780 mg NH_4-N/L. During preparation, the feed solutions were sparged with N_2 until the DO concentration was lower than 0.5 mg/L, and bicarbonate added. The solution was fed to the reactors with diaphragm pumps (DME 2−18, Grundfos, Denmark) at 3.6 L/day. No pH control was applied. The applied air pressures ranged from 2.5 to 60 kPa in R1 and 2.5 to 40 kPa in R2. Gas flow was varied from 0.25 to 4.5 L/min in R1, while it was kept at 0.5 L/min in R2.

Characterization of the O_2 Loading to the Reactor. A cycle is defined as an interval of time, Δt, consisting of an aerated period, $\Delta t_{aerobic}$, plus a nonaerated period (no pressure in the aeration module), $\Delta t_{anaerobic}$. The liquid substrate is fed continuously. Defining the aerobic fraction of a cycle as

$$\alpha = \frac{\Delta t_{aerobic}}{\Delta t_{cycle}} = \frac{\Delta t_{aerobic}}{\Delta t_{anaerobic} + \Delta t_{aerobic}} \quad (1)$$

and taking into account the residual O_2 transfer during anaerobic periods (because of back-diffusion of air through the gas offline, ∼10%), the average O_2 loading (L_{O_2}) for one aeration regime is

$$L_{O_2} = L_{O_2 aerobic} \cdot \alpha + L_{O_2 anaerobic} \cdot (1 - \alpha) \quad (2)$$

Therefore, L_{O_2} was sensitive to the value of the gas pressure and the flow rate (defining the loads during aerobic and anaerobic periods) and α. Detailed description of the calculations of these parameters and the processes occurring within a cycle are found in sections 3 and 8 of the Supporting Information.

N_2O Measurements. Microsensors were used to measure N_2O time series within the biofilm-covered fiber bundles and in the bulk liquid phase upon switching from aerated to nonaerated conditions and vice versa. In addition, N_2O concentrations in the bulk liquid were measured with a gas chromatograph equipped with a 63Ni electron capture detector (Agilent GC7890), since the sensitivity of microsensor was not sufficient to detect fluctuations in the bulk. In parallel we took samples in the bulk liquid to analyze for NH_4^+, NO_3^-, and NO_2^- concentrations. Preparation of the N_2O microsensors (*17*), calibration, and microsensor measurement were performed as previously described (*18*).

Biomass. Two different inoculation strategies were applied for the start-up of the MABRs: continuous vs single addition of AnAOB. First, both reactors were initiated with enriched nitrifying biomass obtained from the Lundtofte WWTP (Denmark). After one month of operation, a 0.8 L tubular reactor containing a nonwoven sheet of polyester with enriched AnAOB biomass (removal rate 0.3 g N/L/day) was placed in the recirculation line of R1 for continuous feed of detached AnAOB into the MABR with the recirculated medium and subsequent adhesion on the already existing biofilm. This reactor was detached once AnAOB activity remained stable (185 days after inoculation). R2 was operated in batch mode for 10 days with one AnAOB addition (approximately 150 g of biomass from long-term operated AnAOB reactors) directly into the reactor.

Molecular and Microscopic Inspection of MABR Biofilms. Real-time quantitative PCR (qPCR) and fluorescence in situ hybridization (FISH) analysis were performed on representative samples using standard protocols (*8, 19*) to quantify and visualize active community fractions in the biofilm. Protocol details can be found in sections 12 and 13 of the Supporting Information.

Other Analyses. Filtered samples (0.45 μm pore size syringe filter) were analyzed daily for NO_2^- and weekly for NH_4^+ and NO_3^- concentrations using commercially available test kits (Spectroquant 14776, 00683, 14773; Merck, Germany). One fiber bundle was removed from each reactor after shutdown, and total and volatile suspended solids (TSS and VSS) were measured according to standard methods (*20*).

Results and Discussion

Reactor Operation.

Continuous Aeration. Prior to the onset of the sequential aeration study, both reactors had been subjected to continuous aeration ($P = 10 \pm 5$ kPa, $G = 1 \pm 0.5$ L/min, $L_{NH_4} = 1.3 \pm 5$ g N/L/day, $T = 26$ °C) for 300 days after AnAOB inoculation. Steady state performance was achieved after 120 days (section 6, Supporting Information). N removal efficiencies were significantly different in both reactors, suggesting a strong effect of the inoculation strategy. Even though the surficial O_2 to NH_4^+ load ratio (L_{O_2}/L_{NH_4}) was set at 1.32 during the whole period, ensuring DO limitation and favoring completely autotrophic N removal (*3*), the removal rates remained as low as 0.28 and 0.06 g N/L/day (21% removal efficiency for R1 and 3% for R2). N mass balances based on steady state concentrations (Table S1, Supporting Information) indicated that even though O_2 supply was limited (to support partial nitritation only), NOB activity was estimated to be responsible for converting most of the generated NO_2^- to NO_3^-: 55% and 95% of the produced NO_2^- was oxidized by NOB in R1 and R2 (calculation details in section 5, Supporting Information). Increasing the medium pH to 8.3 (Na_2CO_3 addition, day 247−260), reduction of air pressure to 2.5 kPa (day 240 on), or temperature increase from 26 to 32 °C (day 151 on), did not induce noticeable changes in reactor performance.

Sequential Aeration. Batch perturbations revealed a strategy toward favoring AOB and AnAOB over NOB activity in the reactors: if aeration was resumed after an extended anoxic phase in the reactor, NO_3^- accumulation significantly lagged behind and remained far below NO_2^- accumulation (section 4, Supporting Information). Based on this observation, both reactors were then operated by applying periodic aeration but with continuous substrate feeding. The overall operational objective was still to optimize the N removal of both reactors (high removal efficiencies and rates) by steadily manipulating L_{O_2} (as described) and $L_{NH_4^+}$ (through changes in NH_4^+ concentration) toward $L_{O_2}/L_{NH_4^+}$ values close to 1.73,

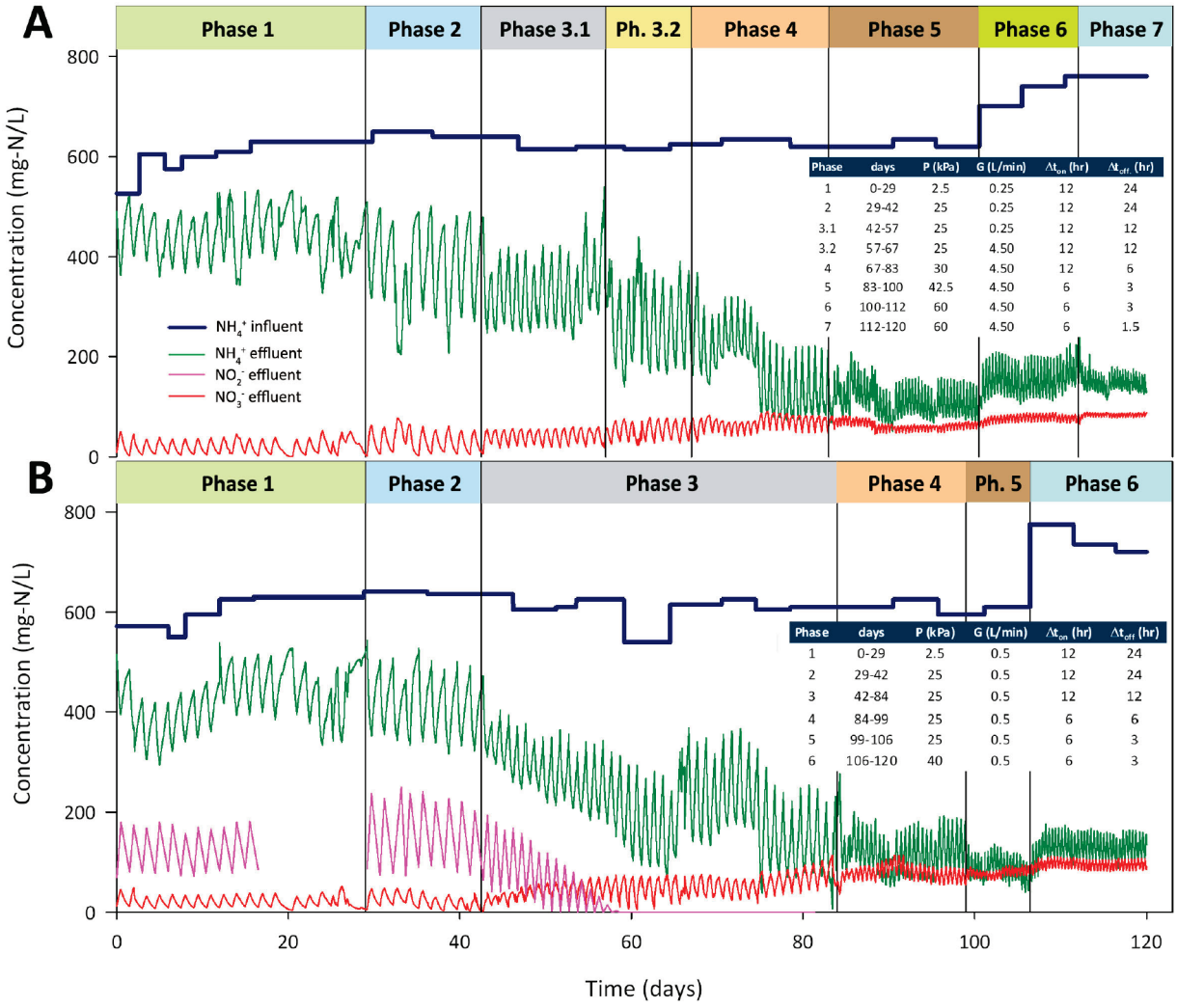

FIGURE 1. Concentrations of N species in the bulk liquid of reactor 1 (A) and reactor 2 (B). Effluent NH_4^+, NO_2^-, and NO_3^- concentrations are presented in dark green, magenta, and red, respectively. Influent NH_4^+ concentration is depicted in dark blue.

the postulated ratio to maximize the removal efficiencies in counter-diffusion biofilm systems (*3*). Details of the operational strategies and performances can be found in section 7 of Supporting Information. Effluent concentrations over time for both reactors are shown in Figure 1A and B for all phases.

In the first phase, the lengths of the aerated and nonaerated periods were set to 12 and 24 h, respectively. Under these conditions, no more than 10% of the overall consumed NH_4^+ (difference between influent and effluent concentration) was converted to NO_3^- at the end of the aerated periods, and most of the generated NO_3^- was washed out during nonaeration. NH_4^+ removal was also observed during the nonaerated periods, due to residual O_2 intrusion in the membrane module (section 8 Supporting Information).

Although L_{O_2} dropped by almost 2/3 in phase 1 (compared to previous continuous aeration), while maintaining L_{NH_4}, average N removal remained very similar in R1 (Figure 2A), and NO_2^- started to accumulate in R2 (Figure 2B). This indicated less DO uptake by NOB and a more desired DO utilization: only 3% and 38% of the produced NO_2^- was now estimated to be metabolized by NOB in R1 and R2 during phase 1 (Table S1, Supporting Information) in contrast to the previous phase. In R1, the NO_2^- was primarily consumed by AnAOB to oxidize NH_4^+, while it accumulated in the bulk liquid of R2 up to 200 mg N/L. The aerobic fractional NO_3^- production (the $\Delta NO_3^-/\Delta NH_4^+$ measured at the end of each aerated period in this phase, section 9, Supporting Information) showed an immediate and slight decrease in both reactors, but still a bit above 0.13, the ratio consistent with AnAOB activity in single-reactor nitritation−Anammox systems (*21*).

With the trends shown in phase 1, the objective of phase 2 was to further increase the N removal in R1 and the NO_2^- production in R2, by increasing the L_{O_2}/L_{NH_4} ratio to 0.78 in R1 and 0.92 in R2, elevating the lumen operating pressure: the expected results were obtained (Figure 2). Even though the aeration intensity of the system was enhanced (and thus the DO at the biofilm/membrane interface), NO_2^- utilization by NOB continued to decline (Table S1, Supporting Information), as well as the $\Delta NO_3^-/\Delta NH_4^+$ ratio, especially in R2 (Figure S6, Supporting Information).

During phase 3, L_{O_2} was further increased by reducing the anaerobic period from 24 to 12 h without changing the total cycle length, resulting in an L_{O_2}/L_{NH_4} ratio of 1.09 and 1.34 in R1 and R2, respectively. This higher O_2 load resulted again in higher NH_4^+ consumption and a clear increased removal efficiency in R1. In R2, three coupled effluent observations clearly revealed the onset of AnAOB activity: a significant decrease in the NH_4^+ levels, the *disappearance* of NO_2^- and no substantial increase in the NO_3^- concentrations. The $\Delta NO_3^-/\Delta NH_4^+$ ratio of the cycles remained similar in R1, while it increased a bit more steeply in R2, probably as side-effect of the appearance of AnAOB activity (about 0.34 at the end of phase 3, Figure S6, Supporting Information). A change in the configuration of the gas line in R1 resulted in a higher

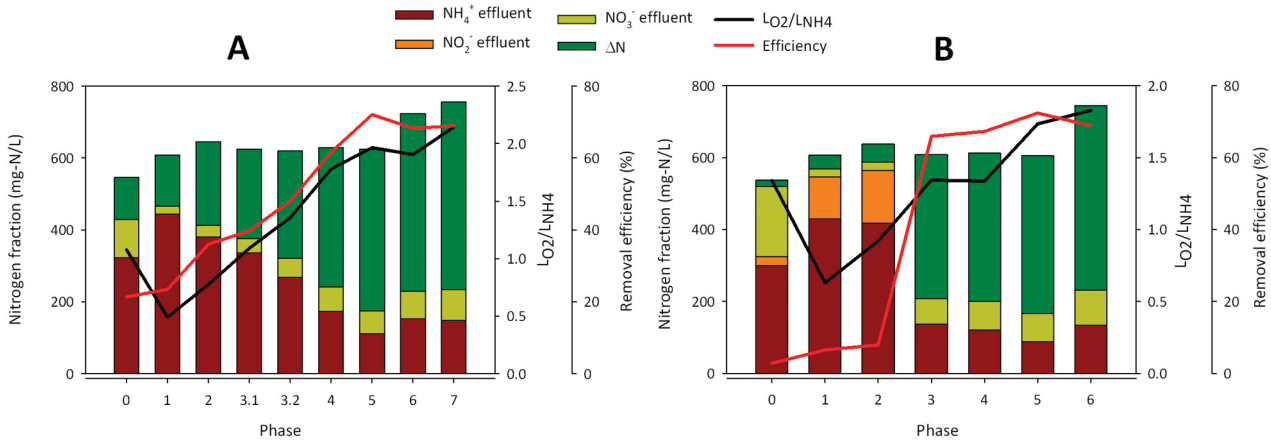

FIGURE 2. Average N balances during the different operational phases for reactor 1 (Panel A) and reactor 2 (Panel B). The total bar height represents the NH_4^+ influent concentration. The color distribution within each bar represents the fraction of each N specie in the effluent at steady state. Sum of effluent NH_4^+ (dark red), NO_2^- (orange), and NO_3^- (pale green) concentrations are subtracted from the influent NH_4^+ concentration to calculate the N removed (ΔN removed, dark green). Phase 0 corresponds to the continuous aeration period. Removal efficiencies and L_{O_2}/L_{NH_4} for each of the phases are read on the right axes.

gas flow rate to the reactor (phase 3.2), increasing the ratio of L_{O_2}/L_{NH_4} and, once more, the reactor removal efficiencies.

Phase 3 was maintained in R2 until steady-state Anammox performance was attained, while the O_2 load to R1 was increased. Once a stable Anammox activity was attained, the performance of R1 and R2 responded very similar to operational changes: removal rates increased by adjusting the L_{O_2}/L_{NH_4} ratios close to the postulated optimum value of 1.73 (Figure 2, Table S1, Supporting Information) (*3*). This ratio was gradually achieved by increasing L_{O_2} (phases 4, 5, and 7 in R1 and phase 5 in R2) or a simultaneous increment of L_{O_2} and L_{NH_4} loads (phase 6 in R1 and R2). Increasing the number of cycles per day, at the same average O_2 and NH_4^+ load (phases 3 and 4, R2, did not affect reactor performance significantly. None of these variations affected the fractional NO_3^- production, which remained on average 0.22 in R1 and 0.35 in R2 (Figure S6, Supporting Information). These values are above the stoichiometric value for Anammox in single-reactor nitritation−Anammox systems, indicating the ongoing contribution of nitratation (*21*). However, the fraction of NO_2^- consumed by NOB during periodic aeration (Table S1, Supporting Information) remained below 9% for both reactors once AnAOB activity was established (from phase 1 and 3 in R1 and R2, respectively), in contrast to the 85% maximum value observed in our reactors during continuous aeration. DO remained mainly below 0.5 mg/L and pH ranged between 6.71−8.31 in the bulk of both reactors throughout the study.

The repression of NOB and emergence of AnAOB activity upon onset of sequential aeration was remarkable. While these conditions may have provided an increased fitness to AnAOB, and as competitors for NO_2^-, may have driven selection against NOB (*14, 22*), it does not explain the initial drop in NOB activity in R2, where little or inexistent Anammox was deduced at the onset of sequential aeration. Instead, direct inhibition of NOB is more plausible. It has been postulated that AOB can excrete hydroxylamine when O_2 supply is suddenly stopped (*23*), a compound inhibitory to NOB (at concentrations as low as 0.35 mg/L) (*24*). Also, AOB produce toxic nitric oxide (NO) when performing denitrification under O_2 limited or anaerobic conditions (*25, 26*). Hence, we speculate that imposition of periodic aeration caused one or more byproducts to be excreted by AOB, which displayed an inhibitory effect against NOB. Definitive proof is required to identify the responsible compound and mechanism.

The highest attained removal efficiencies were 72% at an L_{O_2}/L_{NH_4} ratio of 1.96 for R1 (phase 5) and 1.73 for R2 (phase 5), compared to a theoretical maximum efficiency of 89% derived from theoretical AnAOB stoichiometry (*27*). The higher optimum L_{O_2}/L_{NH_4} in R1 would suggest higher NOB activity than in R2. However, further analysis of the aerobic fractional NO_3^- production in both reactors appears to be in conflict with this observation (much higher in R2 than in R1). Thus, heterotrophic activity may have had a significant role in the N removing processes without significantly affecting the removal efficiency, especially in R1, which would contradict earlier model-based predictions, indicating that operation at loads above 3 g N/m^2/day would significantly reduce N removal efficiency because of heterotrophic growth on decay products (*1*).

Pressures above 60 and 40 kPa did not produce any remarkable change in the performances of R1 or R2 neither in the value of any operational parameter, for example, pH, DO, or N species concentrations. NH_4^+ concentrations were not lower than 100 mg N/L at any time during the phases with such high pressures. With such concentrations and a maximum estimated biofilm thickness of 500 μm (section 14, Supporting Information) model-based calculations suggest that the N removal rates are unlikely to be limited by the lack of NH_4^+ in the deeper biofilm layers and a further increase in the removal rates would have been expected with higher L_{O_2}. Therefore, it appears that the experiment was limited by the ability of the system to provide more O_2. This hypothesis was later confirmed during the disassembly of the reactors, when air leakage through the potting of the fibers was detected.

The maximum N removal rates observed in the present study combine both high volumetric and surficial removal rates and an excellent removal efficiency (0.78 g N/L/day or 5.53 g N/m^2/day, 72% efficiency), which is rare in the literature. More in detail, volumetric and surficial removal rates in other single-reactor autotrophic N removal systems like MBBRs, RDCs, and SBRs, are in the range of 0.06−1 g N/L/day and 2−8.3 g N/m^2/day (*26, 28−34*). Moreover, our maximum removal rate is also above the rate of 0.73 g N/L/day reported for a single-reactor MABR system operated at higher temperatures and for much shorter time showing N removal (40 days) (*35*). MABRs that are operated for N removal via the traditional nitrification/denitrification route with organic carbon, also have lower removal rates (0.05−0.224 g N/L/day or 1.46−4.48 g N/m^2/day) than those reported here (*36−38*).

Periodic aeration has previously been reported as a tool to achieve completely autotrophic N removal (*31, 39*) in SBR configuration. In these cases, very frequent cycling between

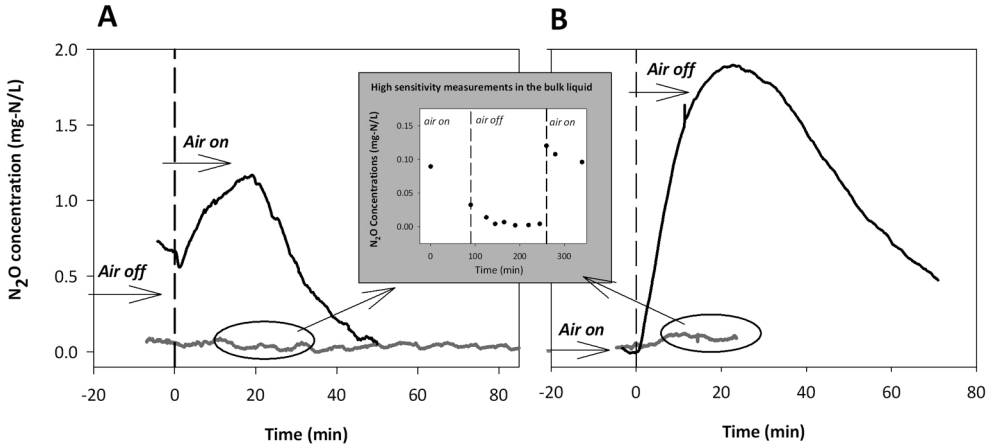

FIGURE 3. Time series N_2O concentrations during dynamic aeration. N_2O was measured with microsensors within bundles (black) and in the bulk medium (gray). Panel (A) shows transition from nonaerated to aerated conditions and (B) from aerated to nonaerated conditions. Conditions switched at time 0. Inset shows high sensitivity GC N_2O measurements in the bulk liquid during different aeration phases.

TABLE 1. Evolution of 16S rRNA Gene Copy Numbers of AOB, NOB, and AnAOB versus Total Bacteria

		16S rRNA gene copy number [copies/ng DNA]					relative abundance[b] [%]			
	months	AOB	AnAOB	*Nitrobacter*	*Nitrospira*	total bacteria	AOB	AnAOB	*Nitrobacter*	*Nitrospira*
R1	0	4.48×10^4 (1.53×10^2)[a]	6.30×10^4 (6.51×10^3)	2.30×10^3 (1.34×10^2)	below detection limit	2.19×10^5 (8.08×10^3)	20.4	28.7	1.05	
	2	4.95×10^4 (8.45×10^3)	1.11×10^5 (1.00×10^4)	1.07×10^4 (1.53×10^2)	1.02×10^1 (6.65×10^0)	2.24×10^5 (3.51×10^3)	22.1	49.5	4.78	0.005
	4	1.89×10^5 (1.31×10^1)	6.54×10^4 (7.17×10^3)	1.90×10^3 (1.47×10^2)	1.28×10^2 (4.59×10^1)	4.51×10^5 (1.58×10^4)	41.8	14.5	0.42	0.028
R2	0	1.56×10^5 (8.33×10^3)	4.51×10^3 (5.90×10^2)	6.58×10^3 (5.04×10^2)	3.63×10^1 (1.16×10^1)	2.09×10^5 (3.51×10^3)	74.6	2.16	3.15	0.017
	2	8.65×10^4 (1.53×10^4)	1.61×10^5 (2.16×10^4)	3.01×10^3 (1.13×10^2)	Below detection limit	2.59×10^5 (6.36×10^3)	33.5	62.4	1.16	0.003
	4	8.07×10^4 (2.31×10^2)	1.62×10^5 (8.02×10^3)	1.62×10^3 (4.58×10^1)	Below detection limit	2.27×10^5 (1.94×10^3)	35.6	71.3	0.71	0.002

[a] Values in parentheses represent standard deviation. [b] Based on the simplified assumption that all taxa have one rRNA operon per cell.

aerated and nonaerated conditions was necessary to attain maximum removal rates of 0.6−0.7 g N/L/day. In opposition to what is presented here, NO_2^- was generated in the aerobic periods and consumed in the anaerobic ones (simultaneous removal could not be established). Hence, with MABRs, NH_4^+ can be continuously converted to N_2 in a single step, yielding effluent concentrations inside a very narrow range by minimizing the length of the nonaerated periods once N removal is established.

In previous experiences with similar MABRs operated at much higher $L_{NH_4^+}$ (*40*), it was observed that concentrations of 3.5 mg O_2/L in the membrane wall and lumen air pressures of 35 kPa were the threshold values to ensure nitritation (and avoid nitratation) on carbon-limited wastewaters. Under these conditions, maximum NO_2^- productions of 1 g N/m^2/day were attained. O_2 loadings above these values resulted in NO_3^- accumulation and lower NO_2^- production fluxes. Here, we show that by periodic aeration, pressures up to 60 kPa (and thus, higher O_2 fluxes) in the same type of membranes can be accommodated to support AnAOB activity and NO_2^- production fluxes of up to 3.15 g N/m^2/day (derived from AnAOB stoichiometry at the maximum observed removal efficiency). Also, the elevated NO_2^- concentration, which preceded the onset of AnAOB activity in R2 (over 200 mg N/L) and DO bulk concentrations (with isolated peaks up to 1.5 mg/L), were much higher than values reported as inhibitory for AnAOB (*7*).

N_2O Turnover in MABRs during Complete Autotrophic N Removal. After assessment of the effect of periodic aeration on reactor performance (phase 7), formation of N_2O during a typical cycle (N load of 1.12 g N/L/day as NH_4^+) was investigated in R1. High-sensitivity GC-measurements showed that N_2O accumulated to ∼0.1 mg N/L in the bulk liquid during the aerated phase and was below the detection limit (<0.0066 mg N/L) during the nonaerated one (Figure 3, inset). With an influent concentration of 750 mg NH_4^+/L, the loss of N_2O from the reactor was ∼0.015% and <0.001% N-N_2O/N-load during the aerated and nonaerated phase, respectively. These values are ∼100 fold lower than emission values reported for full-scale Anammox-nitritation reactors, which range from 1.2 to 2−3% N-N_2O/N-load (*4*) (*41*).

With microelectrode measurements we were able to observe transient formation of N_2O within the biofilm bundles upon switching off the O_2 supply with a maximum of ∼1.96 mg N/L within 20 min (Figure 3B). The N_2O concentration stabilized after 1−1.5 h at ∼0.56 mg N/L. Upon resupply of O_2, the N_2O concentration increased again temporarily within 20 min to a maximum of ∼1.12 mg N/L, followed by a decline within 30 min to concentrations at the detection limit (∼ 0.14 mg N L^{-1}) (Figure 3A). In contrast, the changes in the bulk liquid remained within the range of the detection limit of the microsensors (0.01 mg N-N_2O/L), which is consistent with the GC measurements. N_2O microprofiles showed N_2O production inside and consumption on the outside of the bundles under nonaerated conditions, whereas N_2O was not detected inside the bundles under aerated conditions (section 10−11, Supporting Information).

The results suggest that the dynamic decrease of DO leads to the transient formation of N_2O by AOB inside the biofilm. This is in agreement with previous studies which have shown that AOB in mixed culture biofilms transiently produce N_2O upon dynamic decreases of O_2 (*18, 25*). These studies also showed that formation of N_2O is always coupled to the formation of toxic NO. Thus, the observed transient formation of N_2O supports our hypothesis on the production of an inhibitory compound for NOB by AOB due to the sequential aeration regime.

Because of the establishment of DO gradients, the outermost parts of the biofilm remained anoxic under both aeration and nonaeration conditions. This allowed the establishment of a stable N_2O reduction zone which minimized N_2O loss into the bulk liquid and thus minimized the loss of N_2O from the reactor (Figure 3 inset and sections 10−11, Supporting Information). Consistent with this hypothesis, we measured a net-potential N_2O uptake rate of 0.015 mg N/min/g-VSS reactor biomass in a batch incubation experiment (Figure S8, Supporting Information). Under aerated conditions, the outer anoxic zone of the biofilm is likely to decrease, reducing the N_2O uptake rate and slightly increasing N_2O loss into the bulk compared to nonaerated conditions (Figure 3, inset). In addition, heterotrophic denitrifiers might contribute to N_2O formation under stable nonaerated conditions inside the bundles (Figure S7, Supporting Information) (*18*) or during the shift from aerated to nonaerated conditions as N_2O reductase is the first enzyme of the denitrification apparatus that is inhibited by O_2 (*42*).

Microbial Community Abundance, Composition and Evolution. qPCR was carried out to quantify relative abundance of AOB, NOB and AnAOB before and after implementation of sequential aeration (Table 1). Overall, the copy numbers of 16S rRNA gene ranged from 10^4 to 10^5 for AOB, 10^3 to10^5 for AnAOB, 10^3 to 10^4 for *Nitrobacter* and 10^0 to10^2 for *Nitrospira*. AOB and AnAOB made up the largest fraction of the total community, compared to earlier studies (*43*) indicating very successful enrichment. Before sequential aeration, AOB and AnAOB fractions were 20% and 28% in R1, and 74% and 2% in R2, respectively. After two months of sequential aeration, the AnAOB fraction in R1 increased to 50%, with little change in AOB abundance. Despite a decrease in AnAOB abundance to approximately 40% after four months, the sum of AOB and AnAOB accounted for about 60%, indicating their dominance in the biofilm. NOB abundance, which was dominated by *Nitrobacter* over *Nitrospira* by 10- to 1000-fold, decreased in both R1 and R2. In R2, AnAOB density dramatically increased (36 fold) during four months, reaching relative AnAOB abundance of 71% in R2, concomitant with a significant increase in N removal rate and efficiency (Table S1, Supporting Information). The increase in AnAOB abundance in R2 mirrored the NOB abundance (mainly *Nitrobacter*). Nevertheless, NOB were not completely eliminated from the biofilms in either R1 or R2 likely because of the inherent MABR biofilm geometry, where the innermost region receives high DO and NO_2^- concentrations suitable for NOB growth (*1*). FISH inspection qualitatively matched these observations: AnAOB were easily detected as cluster-like structures located adjacent to AOB clusters as previously reported (*44*), with NOB still detectable as single-scattered cells after 4 months of sequential aeration (Figures S11 and S12, Supporting Information). The outcompetition of AnAOB over NOB for NO_2^-, observed in both reactors, is supported by the low fractional NO_3^- recovery (Figure S6, Supporting Information), indicating that nitritation/anaerobic NH_4^+ oxidation is the main N removal pathway. In sum, the dramatic increase in N removal triggered by the onset of sequential aeration was consistent with an increase in AnAOB abundance.

Acknowledgments

This work was financially supported by the Danish Agency for Science Technology and Innovation (FTP-ReSCoBiR), a Marie Curie Excellence grant (EC Framework Program 6) to B.F.S., a DTU PhD fellowship grant to S.L., and a China Scholarship Council fellowship to S.P.S.

Appendix A

List of Abbreviations

Anammox	anaerobic ammonium oxidation
AnAOB	anaerobic ammonium oxidizing bacteria
AOB	aerobic ammonium oxidizing bacteria
DO	dissolved oxygen
FISH	fluorescence in situ hybridization
G	gas flow rate (L min^{-1})
L_{NH_4}	daily averaged ammonium surface load (g N m^{-2} d^{-1})
L_{O_2}	daily averaged oxygen surface load (g O_2 m^{-2} d^{-1})
MABR	membrane-aerated biofilm reactor
N	nitrogen
N_2	nitrogen gas
N_2O	nitrous oxide
NH_4^+	ammonium
NO	nitric oxide
NO_2^-	nitrite
NO_3^-	nitrate
NOB	nitrite oxidizing bacteria
O_2	oxygen
P	gas pressure (kPa)
qPCR	real-time quantitative polymerase chain reaction
TN	total nitrogen (mg-N·L^{-1})
WWTP	wastewater treatment plant
α	aerated fraction of the total cycle length
$\Delta NO_3^-/\Delta NH_4^+$ ratio	aerobic fractional NO_3^- production ratio measured at the end of each aerated period
Δt	total duration of a cycle (h)
$\Delta t_{aerobic}$	duration of aerated period in one cycle (h)
$\Delta t_{anaerobic}$	duration of nonaerated period in one cycle (h)

Supporting Information Available

Description of the physical and hydrodynamic properties of the setup, operational data not shown in the main manuscript, calculations, data on the N_2O production and consumption, a description of the qPCR and FISH protocols, and FISH results. This information is available free of charge via the Internet at http://pubs.acs.org/.

Literature Cited

(1) Lackner, S.; Terada, A.; Smets, B. F. Heterotrophic activity compromises autotrophic nitrogen removal in membrane-aerated biofilms: Results of a modeling study. *Water Res.* **2008**, *42* (4−5), 1102–1112.

(2) Syron, E.; Casey, E. Membrane-aerated biofilms for high rate biotreatment: Performance appraisal, engineering principles, scale-up, and development requirements. *Environ. Sci. Technol.* **2008**, *42* (6), 1833–1844.

(3) Terada, A.; Lackner, S.; Tsuneda, S.; Smets, B. F. Redox-stratification controlled biofilm (ReSCoBi) for completely autotrophic nitrogen removal: The effect of co-versus counter-diffusion on reactor performance. *Biotechnol. Bioeng.* **2007**, *97* (1), 40–51.

(4) Kampschreur, M. J.; Temmink, H.; Kleerebezem, R.; Jetten, M. S. M.; van Loosdrecht, M. C. M. Nitrous oxide emission during wastewater treatment. *Water Res.* **2009**, *43* (17), 4093–4103.

(5) Stein, L. Y.; Yung, Y. L. Production, isotopic composition, and atmospheric fate of biologically produced nitrous oxide. *Annu. Rev. Earth Planet. Sci.* **2003**, *31*, 329–356.

(6) de Graaf, A. A. V.; de Bruijn, P.; Robertson, L. A.; Jetten, M. S. M.; Kuenen, J. G. Autotrophic growth of anaerobic ammonium-oxidizing micro-organisms in a fluidized bed reactor. *Microbiology* **1996**, *142*, 2187–2196.

(7) Strous, M.; Kuenen, J. G.; Jetten, M. S. M. Key physiology of anaerobic ammonium oxidation. *Appl. Environ. Microbiol.* **1999**, *65* (7), 3248–3250.

(8) Terada, A.; Lackner, S.; Kristensen, K.; Smets, B. F., Inoculum effects on community composition and nitritation performance of autotrophic nitrifying biofilm reactors with counter-diffusion geometry. *Environ. Microbiol.* **2010**, DOI: 10.1111/j.1462-2920.2010.02267.x.

(9) Wang, R. C.; Terada, A.; Lackner, S.; Smets, B. F.; Henze, M.; Xia, S. Q.; Zhao, J. F. Nitritation performance and biofilm development of co- and counter-diffusion biofilm reactors: Modeling and experimental comparison. *Water Res.* **2009**, *43* (10), 2699–2709.

(10) Lackner, S.; Terada, A.; Horn, H.; Henze, M.; Smets, B. F., Performance in Membrane Aerated Biofilm Reactors differs from conventional biofilm systems. *Water Res.* **2010**, DOI: 10.1016/j.watres.2010.07.074.

(11) Blackburne, R.; Yuan, Z. G.; Keller, J. Partial nitrification to nitrite using low dissolved oxygen concentration as the main selection factor. *Biodegradation* **2008**, *19* (2), 303–312.

(12) Ciudad, G.; Gonzalez, R.; Bornhardt, C.; Antileo, C. Modes of operation and pH control as enhancement factors for partial nitrification with oxygen transport limitation. *Water Res.* **2007**, *41* (20), 4621–4629.

(13) Kim, D.-J.; Lee, D.-I.; Keller, J. Effect of temperature and free ammonia on nitrification and nitrite accumulation in landfill leachate and analysis of its nitrifying bacterial community by FISH. *Bioresour. Technol.* **2006**, *97* (3), 459–468.

(14) Wiesmann, U. Biological nitrogen removal from wastewater. In *Advances in Biochemical Engineering/Biotechnology*; Fiechter, A., Ed.; Springer-Verlag: Berlin, 1994; Vol. 51, pp 113−154.

(15) Pollice, A.; Tandoi, V.; Lestingi, C. Influence of aeration and sludge retention time on ammonium oxidation to nitrite and nitrate. *Water Res.* **2002**, *36* (10), 2541–2546.

(16) Hidaka, T.; Yamada, H.; Kawamura, M.; Tsuno, H. Effect of dissolved oxygen conditions on nitrogen removal in continuously fed intermittent-aeration process with two tanks. *Water Sci. Technol.* **2002**, *45* (12), 181–188.

(17) Andersen, K.; Kjaer, T.; Revsbech, N. P. An oxygen insensitive microsensor for nitrous oxide. *Sens. Actuators B Chem* **2001**, *81* (1), 42–48.

(18) Schreiber, F.; Loeffler, B.; Polerecky, L.; Kuypers, M. M. M.; de Beer, D. Mechanisms of transient nitric oxide and nitrous oxide production in a complex biofilm. *ISME J.* **20093**, (11), 1301–1313.

(19) Harper, W. F.; Terada, A.; Poly, F.; Le Roux, X.; Kristensen, K.; Mazher, M.; Smets, B. F. The effect of hydroxylamine on the activity and aggregate structure of autotrophic nitrifying bioreactor cultures. *Biotechnol. Bioeng.* **2009**, *102* (3), 714–724.

(20) APHA. *Standard Methods for the Examination of Water and Wastewater*, 15th ed.; American Public Health Association: Washington, DC, 1980.

(21) Third, K. A.; Sliekers, A. O.; Kuenen, J. G.; Jetten, M. S. M. The CANON system (completely autotrophic nitrogen-removal over nitrite) under ammonium limitation: Interaction and competition between three groups of bacteria. *Syst. Appl. Microbiol.* **2001**, *24* (4), 588–596.

(22) Hao, X. D.; Heijnen, J. J.; van Loosdrecht, M. C. M. Sensitivity analysis of a biofilm model describing a one-stage completely autotrophic nitrogen removal (CANON) process. *Biotechnol. Bioeng.* **2002**, *77* (3), 266–277.

(23) Kostera, J.; Youngblut, M. D.; Slosarczyk, J. M.; Pacheco, A. A. Kinetic and product distribution analysis of NO center dot reductase activity in Nitrosomonas europaea hydroxylamine oxidoreductase. *J. Biol. Inorg. Chem.* **2008**, *13* (7), 1073–1083.

(24) Noophan, P.; Figueroa, L. A.; Munakata-Marr, J. Nitrite oxidation inhibition by hydroxylamine: experimental and model evaluation. *Water Sci. Technol.* **2004**, *50* (6), 295–304.

(25) Kampschreur, M. J.; Tan, N. C. G.; Kleerebezem, R.; Picioreanu, C.; Jetten, M. S. M.; Loosdrecht, M. C. M. Effect of dynamic process conditions on nitrogen oxides emission from a nitrifying culture. *Environ. Sci. Technol.* **2008**, *42* (2), 429–435.

(26) Schmidt, I.; Sliekers, O.; Schmid, M.; Bock, E.; Fuerst, J.; Kuenen, J. G.; Jetten, M. S. M.; Strous, M. New concepts of microbial treatment processes for the nitrogen removal in wastewater. *FEMS Microbiol. Rev.* **2003**, *27* (4), 481–492.

(27) Strous, M.; Heijnen, J. J.; Kuenen, J. G.; Jetten, M. S. M. The sequencing batch reactor as a powerful tool for the study of slowly growing anaerobic ammonium-oxidizing microorganisms. *Appl. Microbiol. Biotechnol.* **1998**, *50* (5), 589–596.

(28) Wett, B. Solved upscaling problems for implementing deammonification of rejection water. *Water Sci. Technol.* **2006**, *53* (12), 121–128.

(29) Vlaeminck, S. E.; Terada, A.; Smets, B. F.; Van der Linden, D.; Boon, N.; Verstraete, W.; Carballa, M. Nitrogen removal from digested black water by one-stage partial nitritation and anammox. *Environ. Sci. Technol.* **2009**, *43* (13), 5035–5041.

(30) Vazquez-Padin, J.; Fernadez, I.; Figueroa, M.; Mosquera-Corral, A.; Campos, J. L.; Mendez, R. Applications of Anammox based processes to treat anaerobic digester supernatant at room temperature. *Bioresour. Technol.* **2009**, *100* (12), 2988–2994.

(31) Third, K. A.; Paxman, J.; Schmid, M.; Strous, M.; Jetten, M. S. M.; Cord-Ruwisch, R. Enrichment of anammox from activated sludge and its application in the CANON process. *Microb. Ecol.* **2005**, *49* (2), 236–244.

(32) Szatkowska, B.; Cema, G.; Plaza, E.; Trela, J.; Hultman, B. A one-stage system with partial nitritation and Anammox processes in the moving-bed biofilm reactor. *Water Sci. Technol.* **2007**, *55* (8−9), 19–26.

(33) Sliekers, A. O.; Third, K. A.; Abma, W.; Kuenen, J. G.; Jetten, M. S. M. CANON and Anammox in a gas-lift reactor. *FEMS Microbiol. Lett.* **2003**, *218* (2), 339–344.

(34) Pynaert, K.; Smets, B. F.; Wyffels, S.; Beheydt, D.; Siciliano, S. D.; Verstraete, W. Characterization of an autotrophic nitrogen-removing biofilm from a highly loaded lab-scale rotating biological contactor. *Appl. Environ. Microbiol.* **2003**, *69* (6), 3626–3635.

(35) Gong, Z.; Bao, H.; Liu, S.; Furukawa, K.; Yang, F. Characterization of functional microbial community in a membrane-aerated biofilm reactor operated for completely autotrophic nitrogen removal. *Bioresour. Technol.* **2008**, *99* (8), 2749–2756.

(36) Downing, L. S.; Nerenberg, R. Total nitrogen removal in a hybrid, membrane-aerated activated sludge process. *Water Res.* **2008**, *42* (14), 3697–3708.

(37) Hibiya, K.; Terada, A.; Tsuneda, S.; Hirata, A. Simultaneous nitrification and denitrification by controlling vertical and horizontal microenvironment in a membrane-aerated biofilm reactor. *J. Biotechnol.* **2003**, *100* (1), 23–32.

(38) Terada, A.; Hibiya, K.; Nagai, J.; Tsuneda, S.; Hirata, A. Nitrogen removal characteristics and biofilm analysis of a membrane-aerated biofilm reactor applicable to high-strength nitrogenous wastewater treatment. *J. Biosci. Bioeng.* **2003**, *95* (2), 170–178.

(39) Wett, B. Development and implementation of a robust deammonification process. *Water Sci. Technol.* **2007**, *56* (7), 81–88.

(40) Downing, L. S.; Nerenberg, R. Effect of oxygen gradients on the activity and microbial community structure of a nitrifying, membrane-aerated biofilm. *Biotechnol. Bioeng.* **2008**, *101* (6), 1193–1204.

(41) Kampschreur, M. J.; van der Star, W. R. L.; Wielders, H. A.; Mulder, J. W.; Jetten, M. S. M.; van Loosdrecht, M. C. M. Dynamics of nitric oxide and nitrous oxide emission during full-scale reject water treatment. *Water Res.* **2008**, *42* (3), 812–826.

(42) Otte, S.; Grobben, N. G.; Robertson, L. A.; Jetten, M. S. M.; Kuenen, J. G. Nitrous oxide production by Alcaligenes faecalis under transient and dynamic aerobic and anaerobic conditions. *Appl. Environ. Microbiol.* **1996**, *62* (7), 2421–2426.

(43) Pynaert, K.; Verstraete, W.; Smets, B. F.; Beheydt, D. Start-up of autotrophic nitrogen removal reactors via sequential biocatalyst addition. *Environ. Sci. Technol.* **2004**, *38* (4), 1228–1235.

(44) Tsushima, I.; Ogasawara, Y.; Kindaichi, T.; Satoh, H.; Okabe, S. Development of high-rate anaerobic ammonium-oxidizing (anammox) biofilm reactors. *Water Res.* **2007**, *41* (8), 1623–1634.

ES1013467